Mechanism of Formation of Uniform-Sized Silica Nanospheres Catalyzed by Basic Amino Acids

Toshiyuki Yokoi,[†] Junji Wakabayashi,[‡] Yuki Otsuka,[‡] Wei Fan,[‡,⊥] Marie Iwama,[‡]
Ryota Watanabe,[†] Kenji Aramaki,[§] Atsushi Shimojima,[‡] Takashi Tatsumi,[†] and
Tatsuya Okubo*,[‡]

[†]*Chemical Resources Laboratory, Tokyo Institute of Technology, 4259 Nagatsuta, Midori-ku, Yokohama
226-8503, Japan,* [‡]*Department of Chemical System Engineering, The University of Tokyo, 7-3-1 Hongo,
Bunkyo-ku, Tokyo 113-8656, Japan, and* [§]*Graduate School of Environment and Information Sciences,
Yokohama National University, 79-7 Tokiwadai, Hodogaya-ku, Yokohama 240-8501, Japan.*
[⊥] *Present address: Department of Chemical Engineering and Materials Science, Institute of Technology,
University of Minnesota, 151 Amundson Hall, 421 Washington Avenue SE, Minneapolis, MN 55455*

A liquid-phase method for preparing uniform-sized silica nanospheres (SNSs) 12 nm in size and their three-dimensionally ordered arrangement upon solvent evaporation have recently been pioneered by us. The SNSs are formed in the emulsion system containing $Si(OEt)_4$ (TEOS), water, and basic amino acids under weakly basic conditions (pH 9−10). Here, we report the formation mechanism of the SNSs; the reasons for the uniform size and the ordered arrangement are described in detail. The formation process is monitored by FE-SEM, SAXS, and liquid-state NMR. The FE-SEM observations reveal that silica nanoparticles ca. 4 nm in size are formed in the water phase at the early stage (∼0.5 h) of the reaction. The SAXS measurements suggest that the number density of the particles remains unchanged when they are gradually grown. Liquid-state ^1H NMR analyses suggest that TEOS are slowly hydrolyzed at the oil−water interface to continuously supply silicate species into the water phase. The silicate species are immediately consumed for the growth of the parent particles without forming new particles. The size of the SNSs can be tuned from 8 to 35 nm by varying the synthesis conditions and/or the amount of TEOS. The zeta potential and pH of the dispersion of SNSs throughout the solvent evaporation process are almost constant approximately at −40 mV and 9−10, respectively; the SNSs have been well-dispersed until the final stage of the evaporation process. The critical roles of basic amino acids in the formation and regular arrangement of SNSs are discussed based on the experimental results.

1. Introduction

Silica is a fundamental mineral commonly found in nature and has been widely used in industrial fields.[1,2] Colloidal silica spheres uniform in size and shape have been applied as optical filters, pharmaceutical binders, photographic emulsions, chromatographic agents, sensing elements, catalysts, chemical and mechanical polishing materials, stabilizers, coating layers, and so on.[3−6] The Stöber method is well-known to produce colloidal silica spheres by hydrolysis and condensation of silicon alkoxides (e.g., tetraethyl orthosilicate $Si(OC_2H_5)_4$, abbreviated hereafter as TEOS) in alcohol solvents (e.g., ethanol) in the presence of water and a base catalyst (e.g., NH_3).[7−10] Up to now, extensive studies have been conducted on the formation mechanism,[11] surface modification,[12,13] and fabrication of self-assembled (opal) thin

*Corresponding author. Phone: 81-3-5841-7348. Fax: 81-3-5800-3806. E-mail: okubo@chemsys.t.u-tokyo.ac.jp.

(1) Iler,R. K. The Chemistry of Silica; Wiley: New York, 1978.
(2) (a) Brinker, C. J. *J. Non-Cryst. Solids* **1988,** *100,* 31–50. (b) Brinker, C. J.; Scherer,G. W. Sol−Gel Science; Elsevier: Amsterdam, 1990.
(3) Unger, K. K.; Kumar, D.; Grün, M.; Büchel, G.; Lüdtke, S.; Adam, Th.; Schumacher, K.; Renker, S. *J. Chromatography A* **2000,** *892,* 47–55.
(4) Gosa, K. L.; Uricanu, V. *Colloids Surf., A* **2002,** *197,* 257–269.
(5) Leder, G.; Ladwig, T.; Valter, V.; Frahn, S.; Meyer, J. *Prog. Org. Coatings* **2002,** *45,* 139–144.
(6) Adl, S.; Rahman, I. A. *Ceram. Inst.* **2001,** *27,* 681–687.

(7) Stöber, W.; Fink, A. *J. Colloid Interface Sci.* **1968,** *26,* 62–69.
(8) (a) Van Helden, A. K.; Jansen, J. W.; Vrij, A. *J. Colloid Interface Sci.* **1981,** *81,* 354–368. (b) Van Blaaderen, A.; Van Geest, J.; Vrij, A. *J. Colloid Interface Sci.* **1992,** *154,* 481–501.
(9) (a) Matijevic, E. *Acc. Chem. Res.* **1981,** *14,* 22–29. (b) Matijevic, E. *Chem. Mater.* **1993,** *5,* 412–426. (c) Matijevic, E. *Langmuir* **1994,** *10,* 8–16.
(10) Nozawa, K.; Gailhanou, H.; Raison, L.; Panizza, P.; Ushiki, H.; Sellier, E.; Delville, J. P.; Delville, M. H. *Langmuir* **2005,** *21,* 1516–1523.
(11) Bogush, G. H.; Tracy, M. A.; Zukoski, C. F. *J. Non-Cryst. Solids* **1988,** *104,* 95–106.
(12) Suratwala, T. I.; Hanna, M. L.; Miller, E. L.; Whitman, P. K.; Thomas, I. M.; Ehrmann, P. R.; Maxwell, R. S.; Burnham, A. K. *J. Non-Cryst. Solids* **2003,** *316,* 349–363.
(13) Pham, K. N.; Fullston, D.; Sagoe-Crentsil, K. *J. Colloid Interface Sci.* **2007,** *315,* 123–127.

films of the Stöber silica spheres.[14−18] However, this method hardly provides access to uniform-sized silica nanospheres with a size of below 50 nm and their three-dimensionally ordered arrangement, though high-tech industries are developing a tremendous demand for such silica spheres.[10] Although a variety of colloidal silica spheres below 50 nm in size are commercially available, the degree of uniformity has been insufficient.

We have recently developed a simple and novel liquid-phase method for preparing uniform-sized silica nanospheres (SNSs) ca. 12 nm in size.[19,20] The SNSs were synthesized through hydrolysis and condensation reactions of TEOS in the emulsion system containing TEOS, water and basic amino acids such as lysine and arginine under weakly basic conditions (pH 9−10). After the reaction, uniform-sized SNSs were stably dispersed in homogeneous solutions without any precipitation. Interestingly, the arrangement of these SNSs into a cubic closed packed (ccp) structure was achieved simply by solvent evaporation. Thus formed SNSs can be categorized into well-ordered mesoporous silicas because they have three-dimensional, interparticle voids with high uniformity. This route for producing mesoporous materials has been designated as "hard-sphere packing (HSP)" mechanism,[21] which is different from the well-known surfactant-templating route.[22] The resulting SNSs can be used as porous silicas as well as silica matrix; for example, well-ordered SNSs having three-dimensional mesopores can serve as a template for fabricating mesoporous carbon and various metal oxides.

This technique based on the reaction of TEOS in the presence of basic amino acids has attracted increasing attention. Tsapatsis and co-workers reported the preparation of silica nanospheres with a size of ca. 5 nm by addition of TEOS to an unbuffered, aqueous solution of lysine.[23] They also succeeded in the fabrication of multilayer and near-monolayer-ordered coatings of silica nanospheres on a silicon substrate.[24] Most recently, Hartlen et al. reported the synthesis of monodispersed

silica spheres with the size ranging from 15 to 200 nm by employing our method with modifications.[25]

Despite these successes, the formation mechanism of the silica spheres and the role of the basic amino acid have not been fully understood yet. Main differences between the Stöber method and our method are the kind of base and pH in the synthesis system. The reactions in our method proceed in the presence of basic amino acids in place of ammonia; the pHs of the Stöber and our methods are 11−12 and 9−10, respectively. In addition, another difference is that ethanol is usually used as a solvent in the Stöber method, whereas TEOS and water react at the interface without any cosolvents in our method. These differences are important in understanding the formation mechanism of the SNSs. The role of basic amino acids is of particular interest from the viewpoint of bioinspired chemistry. Recent studies have shown that some derivatives of amino acids and certain polypeptides direct the formation of silica unique in size, morphology, and structure.[26−29]

The clarifications of the growth kinetics and the stability of colloidal suspensions are indispensable for the elucidation of their formation mechanisms. For this purpose, several attempts have been made using various instrumental techniques such as dynamic light-scattering (DLS),[30] NMR spectroscopy,[31,32] transmission electron microscopy (TEM),[33] small-angle X-ray scattering (SAXS),[34−40] and fluorescence anisotropy.[41]

Here we report the formation mechanism of uniform-sized SNSs catalyzed by basic amino acids; the reasons for uniform size and well-ordered arrangement as well as the role of basic amino acids are described in detail. Field-emission scanning electron microscopy (FE-SEM),

(14) Okudera, H.; Hozumi, A. *Thin Solid Films* **2003**, *434*, 62–68.
(15) Yin, Y.; Lu, Y.; Gates, B.; Xia, Y. *J. Am. Chem. Soc.* **2001**, *123*, 8718–8729.
(16) Masuda, Y.; Itoh, M.; Yonezawa, T.; Koumoto, K. *Langmuir* **2002**, *18*, 4155–4159.
(17) Szekeres, M.; Kamalin, O.; Grobet, P. G.; Schoonheydt, R. A.; Wostyn, K.; Clays, K.; Persoons, A.; Dékány, I. *Colloids Surf., A* **2003**, *227*, 77–83.
(18) Ko, H.-Y.; Lee, H.-W.; Moon, J. *Thin Solid films* **2004**, *447−448*, 638–644.
(19) Yokoi, T.; Sakamoto, Y.; Terasaki, O.; Kubota, Y.; Okubo, T.; Tatsumi, T. *J. Am. Chem. Soc.* **2006**, *128*, 13664–13665.
(20) Yokoi, T.; Iwama, M.; Watanabe, R.; Sakamoto, Y.; Terasaki, O.; Kubota, Y.; Kondo, J. N.; Okubo, T.; Tatsumi, T. *Stud. Surf. Sci. Catal.* **2007**, *170B*, 1774–1780.
(21) Tang, J.; Zhou, X.; Zhao, D.; Lu, G. Q.; Zou, J.; Yu, C. *J. Am. Chem. Soc.* **2007**, *129*, 9044–9048.
(22) (a) Huo, Q.; Margolese, D. I.; Ciesla, U.; Feng, P.; Gier, T. E.; Sieger, P.; Leon, R.; Stucky, G. D. *Nature* **1994**, *368*, 317–321. (b) Huo, Q.; Margolese, D. I.; Ciesla, U.; Demuth, D. G.; Feng, P.; Gier, T. E.; Sieger, P.; Firouzi, A.; Chmelka, B. F.; Schüth, F.; Stucky, G. D. *Chem. Mater.* **1994**, *6*, 1176–1191.
(23) Davis, T. M.; Snyder, M. A.; Krohn, J. E.; Tsapatsis, M. *Chem. Mater.* **2006**, *18*, 5814–5816.
(24) Snyder, M. A.; Lee, J. A.; Davis, T. M.; Scriven, L. E.; Tsapatsis, M. *Langmuir* **2007**, *23*, 9924–9928.
(25) Hartlen, K. D.; Athanasopoulos, A. P. T.; Kitaev, V. *Langmuir* **2008**, *24*, 1714–1720.
(26) Che, S.; Liu, Z.; Ohsuna, T.; Sakamoto, K.; Terasaki, O.; Tatsumi, T. *Nature* **2004**, *419*, 281–284.
(27) Cha, J. N.; Stucky, G. D.; Morse, D. E.; Deming, T. J. *Nature* **2000**, *403*, 289–292.
(28) Hawkins, K. M.; Wang, S. S.-S.; Ford, D. M.; Shantz, D. F. *J. Am. Chem., Soc.* **2004**, *126*, 9112–9119.
(29) McKenna, B. J.; Birkedal, H.; H; Bartl, M.; Deming, T. J.; Stucky, G. D. *Angew. Chem., Int. Ed.* **2004**, *43*, 5652–5655.
(30) (a) Matsoukas, T.; Gulari, E. *J. Colloid Interface Sci.* **1989**, *124*, 252–261. (b) Matsoukas, T.; Gulari, E. *J. Colloid Interface Sci.* **1989**, *132*, 13–21.
(31) Lee, K.; Look, J.; Harris, M. T.; McCormick, A. V. *J. Colloid Interface Sci.* **1997**, *194*, 78–88.
(32) Bailey, J. K.; Mecartney, M. L. *Colloids Surf.* **1992**, *63*, 151–161.
(33) van Blaaderen, A.; Kentgens, A. P. M. *J. Non-Cryst. Solids* **1992**, *149*, 161–178.
(34) Brinker, C. J.; Keefer, K. D.; Schaefer, D. W.; Assink, R. A.; Kay, B. D.; Ashley, C. S. *J. Non-Cryst. Solids* **1984**, *63*, 45–59.
(35) Keefer, K. D.; Schaefer, D. W. *Phys. Rev. Lett.* **1986**, *56*, 2376–2379.
(36) (a) Boukari, H.; Lin, J. S.; Harris, M. T. *J. Colloid Interface Sci.* **1997**, *194*, 311–318. (b) Boukari, H.; Lin, J. S.; Harris, M. T. *Chem. Mater.* **1997**, *9*, 2376–2384.
(37) Green, D. L.; Lin, J. S.; Lam, Y.-F.; Hu, M. Z.-C.; Schaefer, D. W.; Harris, M. T. *J. Colloid Interface Sci.* **2003**, *266*, 346–358.
(38) Lindner, P.; Zemb, T. Neutrons, X-rays, and Light: Scattering Methods Applied to Soft Condensed Matter, 1st ed.; Elsevier: Amsterdam, 2002.
(39) Guinier, A.; Fournet, G. Small-Angle Scattering of X-rays SAXS; Wiley: New York, 1955.
(40) (a) Glatter, O. *J. Appl. Crystallogr.* **1977**, *10*, 415–421. (b) Glatter, O. *J. Appl. Crystallogr.* **1979**, *12*, 166–175.
(41) Tleugabulova, D.; Duft, A. M.; Zhang, Z.; Chen, Y.; Brook, M. A.; Brennan, J. D. *Langmuir* **2004**, *20*, 5924–5932.

SAXS and liquid-state NMR techniques have been employed for monitoring the reaction of TEOS and the formation of the SNSs. The evaporation process has also been examined and the resulting solid-state SNSs were characterized by solid-state NMR and FE-SEM. Furthermore, the effect of the stirring conditions and the composition of the reactants have been examined in detail.

2. Experimental Section

2.1. Preparations. *2.1.1. Preparation of SNSs.* The SNSs 12 nm in size were synthesized according to the original method with slight modifications.[19] First, regent grade lysine (0.001 mol, Aldrich, 98%) was dissolved in deionized water with stirring at 333 K. TEOS (0.05 mol, Tokyo Kasei) was added to the lysine−water solution in one step. The molar composition of the reactants was $1TEOS: 0.02lysine: 162H_2O$. Note that the pH of this system was 9.4 and that this system consists of two phases at the beginning; one is the water phase containing lysine and the other is the oil phase consisting of unhydrolyzed TEOS. The mixture was stirred at 333 K for 24 h using a magnetic stirrer with a Teflon-coated stirring bar ($15 \times \emptyset 7$ mm) at 550 rpm. The SNSs were also synthesized by varying the stirring rate.

2.1.2. Preparation of SNSs with Varying the Amount of TEOS. The change in the amount of TEOS as a silica source would cause the change in the concentration of the silicate species, leading to the changes in the size as well as uniformity of the spheres. The effect of the amount of TEOS was investigated by means of two methods. One is the change in the initial amount of TEOS (method A); the molar composition of the reactants was $xTEOS: 0.02lysine: 162H_2O$, where $x = 1, 2, 3, 4,$ and 5. When $x > 2$, the stirring time was extended to 48 h so that the reaction of TEOS was completed. The other is the stepwise addition of TEOS into the parent synthesis system after the reaction at 333 K for 12 h (method B). The final molar ratio of the mixture was adjusted to $(1 + y)TEOS: 162H_2O: 0.02lysine$, where $y = 2, 4, 6, 8,$ and 10. Additional TEOS was added in a stepwise manner; the molar ratio of TEOS was $y = 2$ in each step. After the addition of TEOS, the resultant synthesis system was further stirred at 333 K for 24 h.

2.1.3. Preparation of Silica Spheres by the Stöber Method. As a control, silica spheres around 300 nm in size were prepared by the Stöber method.[8−10] TEOS was added into the mixture of water and NH_3 in ethanol with stirring at room temperature. The molar composition was $1TEOS: 2.9NH_3: 18.4H_2O: 100EtOH$. After being stirred at room temperature for 24 h, a colloidal dispersion of the silica spheres was obtained. Finally, the solid-state silica product was recovered by evaporation of the solvents.

2.2. Characterizations of Dispersions at Early Stages of Reaction. The size of the dispersed SNSs in the synthesis system was evaluated by FE-SEM observation on a Hitachi S-5200 without coating; a copper grid was dipped into the emulsion system. Note that in the reaction time of < 1 h, clear, high-magnification images could not be captured because the particles were quickly aggregated.

The SAXS experiments were conducted on a SAXSess (Anton-Paar) system to estimate the number density of the particles. Samples were placed in a vacuum-tight quartz capillary holder 1 mm in diameter and measured at 298 K. A monochromatic, line-collimation source of Cu Kα radiation was used with a 265 mm sample-to-detector distance. The scattering patterns were collected over a 10 min period on a phosphor imaging plate within the Q range of $0.1−8$ nm^{-1}. Patterns were normalized to the height of the primary beam signal using the SAXSquant software. Detailed conditions for SAXS measurements and analyses are described in the Supporting Information.

The kinetics of the synthesis of the SNSs was investigated by liquid-state ^1H- and ^{29}Si NMR. The emulsion system was allowed to stand for several minutes to separate the oil phase containing unhydrolyzed TEOS from the water phase containing SNSs. Samples were obtained from the water phase at the reaction time ranging from 0.5 to 12 h. For this experiment, 20 mol % of H_2O was replaced by D_2O to ensure the deuterium lock, and acetonitrile was added as the internal standard to estimate the concentration of ethanol derived from TEOS hydrolysis. The spectra were recorded on a JEOL EX270 apparatus.

The magnitude of the zeta potential gives an indication of the stability of the colloidal system. The zeta potentials (z) of the silica spheres produced by the Stöber and our methods were monitored throughout the evaporation process on a Zetasiser Nano instrument (Malvern Instruments Ltd.). Detailed conditions for zeta potential measurements and analyses are described in the Supporting Information. The pH of the synthesis system was also monitored throughout the evaporation process.

2.3. Characterizations of SNSs Collected by Centrifugation. The SNSs in the dispersion prepared as mentioned in section 2.1.1. (molar compositions of $1 TEOS: 0.02 lysine: 162H_2O$, after stirring at 550 rpm for 24 h) were forcibly collected by centrifugation at 60 krpm for 30 min. After removal of the supernatant liquid, the resulting clear, transparent gel was put on a filter paper and air-dried at room temperature for 1 day. The resulting white powders were characterized by CHN elemental analysis (Perkin-Elmer 240C elemental analyzer), TG-DTA, and ^{13}C CP/MAS NMR analysis (JEOL-ECA400 spectrometer at 100.6 MHz and a spinning frequency of 4 kHz).

2.4. Characterizations of SNSs after Solvent Evaporation. The dispersions of the SNSs were transferred to an evaporating dish after being kept static at 373 K for 24 h, and then evaporated to dryness in an oven at 373 K, resulting in the formation of white-colored solid SNSs. FE-SEM images of the powder samples were also obtained on a Hitachi S-5200 microscope operated at 30 kV. Solid-state ^{29}Si MAS NMR spectrum was recorded on a JEOL-ECA400 spectrometer at 79.4 MHz and a sample spinning frequency of 5 kHz. Thermogravimetry (TG) and differential thermal analysis (DTA) were performed on a Rigaku PU 4K equipment using a mixture of 10% O_2 and 90% He. The heating rate was set at 10 K/min.

3. Results

3.1. Formation Process of SNSs. Initially, the reaction mixture with a molar composition of $1 TEOS: 0.02$ lysine: $162H_2O$, was an emulsion system; however, it turned into a homogeneous dispersion after being stirred at 333 K for 12 h. Considering the fact that uniform-sized SNSs were already formed at this stage,[19] characterizations of the early stage of the reaction are essential to understand the formation mechanisms. Because the ^{29}Si NMR analysis (data not shown) confirmed that only TEOS was contained in the oil phase, the water phase of the emulsion was mainly characterized at various reaction times after the addition of TEOS.
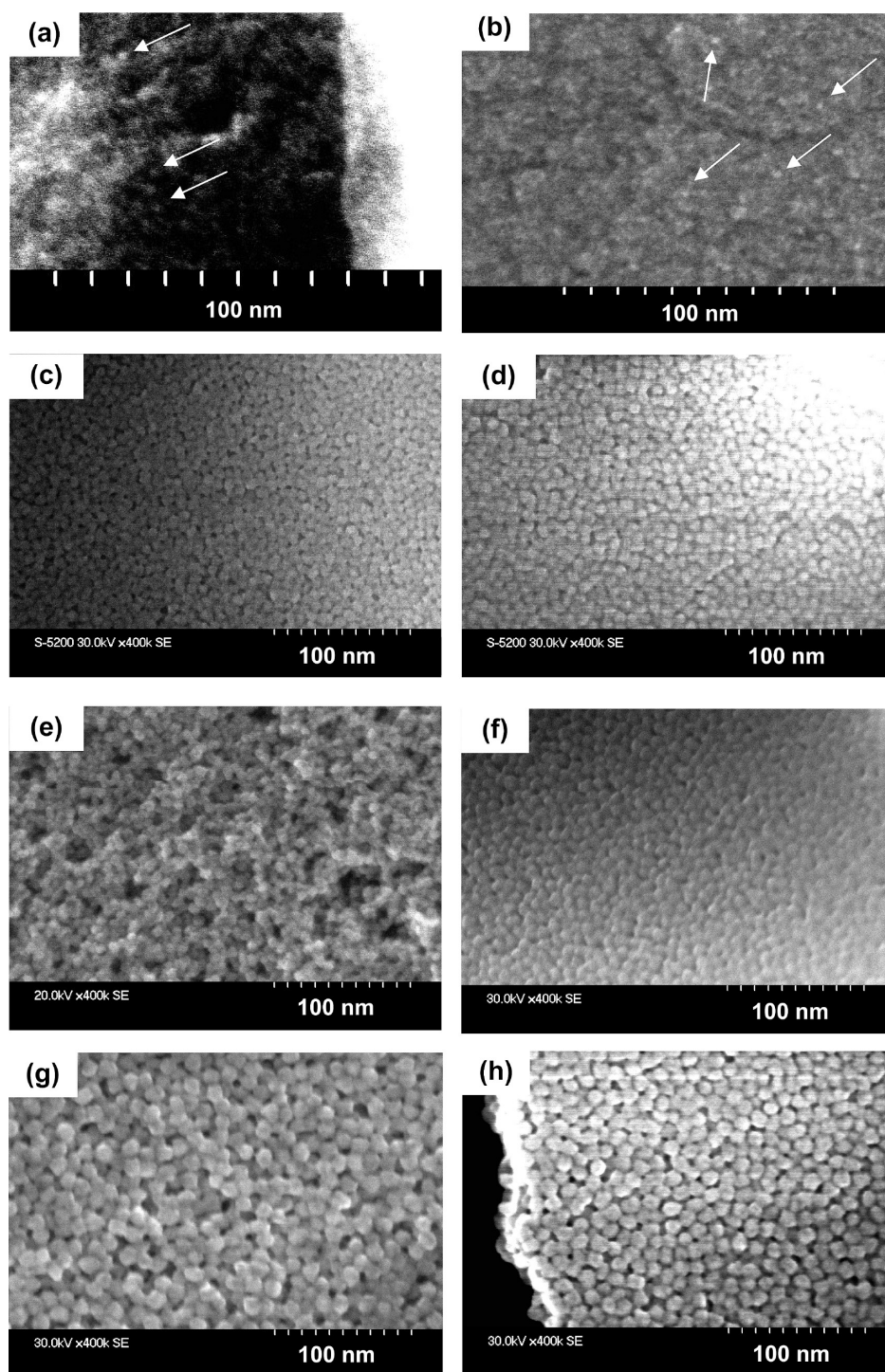
Figure 1. FE-SEM images of the silica products formed after (a) 0.5, (b) 1, (c) 1.25, (d) 1.5, (e) 2, (f) 5, (g) 8, and (h) 24 h of reaction in the system with the molar composition of 1:0.02:162 TEOS:lysine:H_2O.

The FE-SEM observations revealed that uniform-sized silica particles are formed regardless of the reaction time (Figure 1). Typical SEM images of the products after 0.5 and 1 h of the reaction are shown in images a and b in Figure 1, respectively. As indicated by arrows, only a few particles 4−5 nm in size are observed, implying that most of the particles are not formed at these stages. After 1.25 h of the reaction, particles 6 nm in size are clearly observed (Figure 1c). The particle size is increased along with the reaction time; the sizes after 1.5, 2, 5, 8, and 24 h are 7, 7, 9,

12 and 12 nm, respectively. The particle size levels off at ca. 12 nm after 8 h. Assuming that all TEOS are used for the formation of SNSs 12 nm in size, the silica particles 4 and 9 nm in size correspond to ca. 4 and 42% of TEOS added in this system, respectively.

Figure 2a shows the SAXS patterns of the water phase of the emulsion system. The peaks are gradually shifted to lower Q values with an increase in the reaction time from 0.5 to 4 h. The number density (n) of the SNSs was estimated by using the GIFT program to calculate the
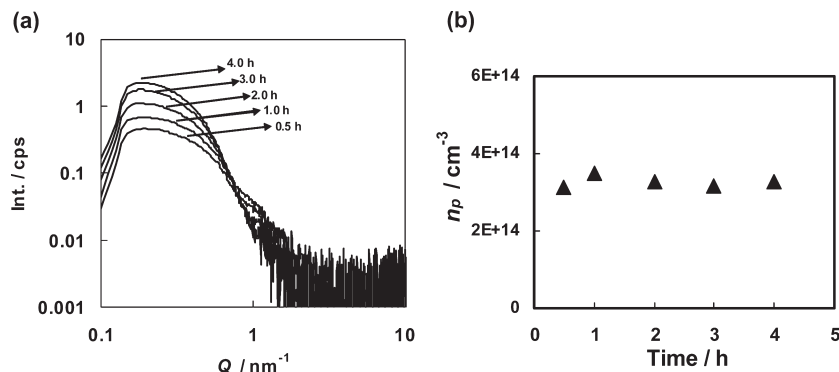
Figure 2. (a) SAXS patterns in the water phase of the emulsion system with the stirring time after the addition of TEOS varied. (b) Plot of the number density (n) in the water phase as a function of the reaction time.
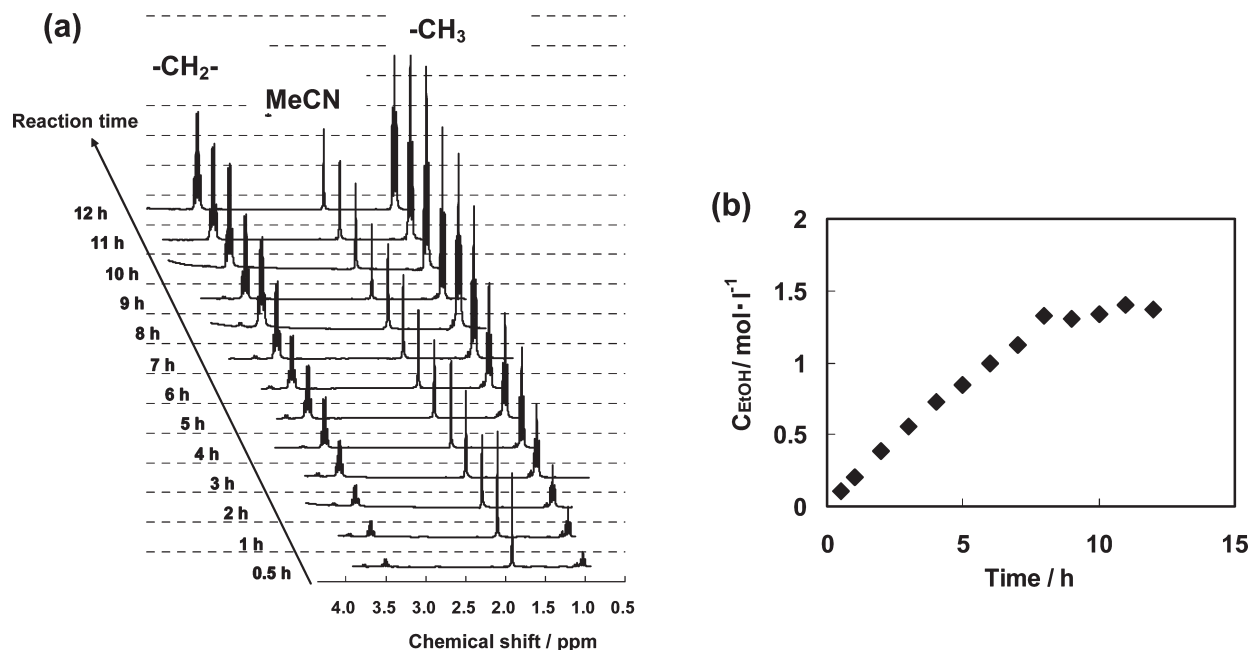

Figure 3. (a) Liquid-state ^{1}H NMR spectra of the water phase in the synthesis system with the stirring time after the addition of TEOS varied. *MeCN was added to the sample as a reference. (b) Relationship between the ethanol concentration (C_{EtOH}) of the water-phase in the synthesis system and the reaction time.

pair distance distribution function (PDDF)[40] and to perform the Guinier analysis,[41] respectively. Figure 2b shows plots of n as a function of the reaction time, confirming that n is almost constant during the whole period. From the FE-SEM and SAXS results, it is suggested that the particle growth proceeded without forming new particles after 0.5 h.

Liquid-state ^{1}H NMR analyses of the water phase in the emulsion system at various stages were conducted to monitor the hydrolysis of TEOS (Figure 3a). The proton signals of ethanol ($-CH_2-$ and $-CH_3$ at at 3.5 ppm and 1.0 ppm, respectively) are increased with increasing time, indicating the progress of TEOS hydrolysis. No signals of ethoxy groups ($\equiv SiOCH_2CH_3$) due to partially hydrolyzed TEOS are observed. Figure 3b shows the relationship between the ethanol concentration (C_{EtOH}) and the reaction time. If all of TEOS is completely hydrolyzed in this system, the C_{EtOH} is supposed to be 1.37 mol L^{-1}. The C_{EtOH} reached ca. 1.36 mol L^{-1} after 8 h of the reaction, implying that TEOS was completely hydrolyzed at this

stage. Actually, we confirmed that the oil phase of TEOS disappeared after 8 h to form a homogeneous dispersion. The C_{EtOH} after 0.5 and 5 h were 0.1 and 0.8 mol L^{-1}, meaning that ca. 7 and 59% of TEOS were consumed, respectively. On the basis of these TEOS consumptions (7 and 59%), the particle sizes are calculated to be 5 and 10 nm, respectively, almost in accordance with the particle sizes evaluated by FE-SEM.

We also performed the liquid-state ^{29}Si NMR analysis of the water phases after 0.5 and 3 h of the reaction; however, no signals of dissolved silicate species including completely hydrolyzed monomer and oligomers were observed. Note that the resonances from silica particles are hardly detected because of the longer relaxation time that is common for the ^{29}Si nuclei in solids. Thus the concentration of dissolved silicate species was very low in the water phase of the emulsion system, which is consistent with the report by Iler and his co-workers that the silica solubility is exceedingly low at pH 9−10.[1]
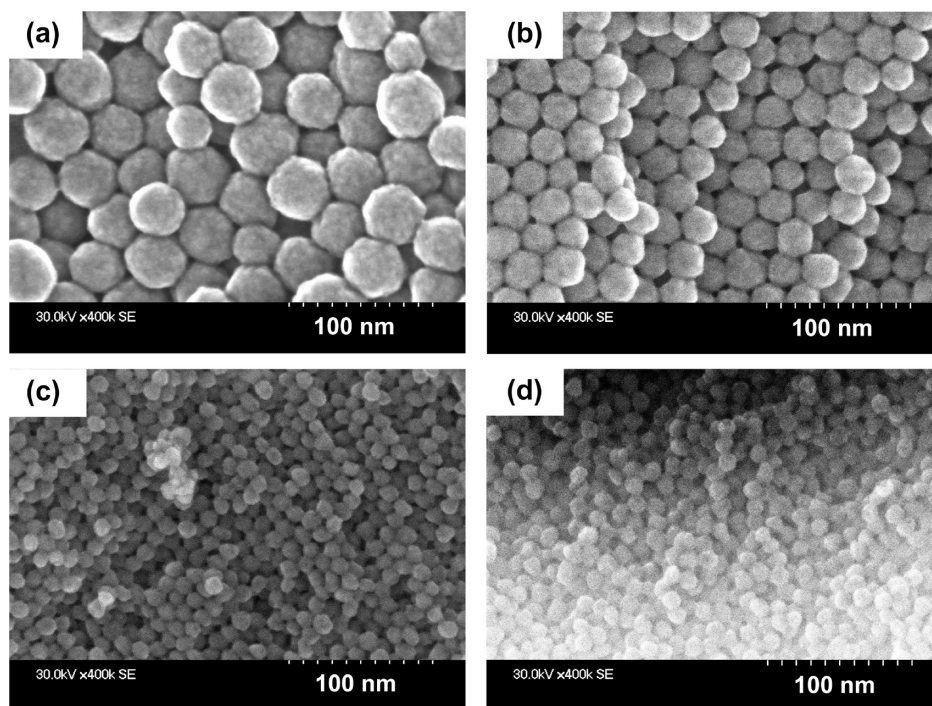
Figure 4. FE-SEM images of the silica nanospheres (SNSs) synthesized with various stirring rates: (a) 0 (static condition), (b) 150, (c) 550, and (d) 950 rpm. Scale bar: 100 nm. The dispersions of the SNSs were evaporated to dryness before the observation.
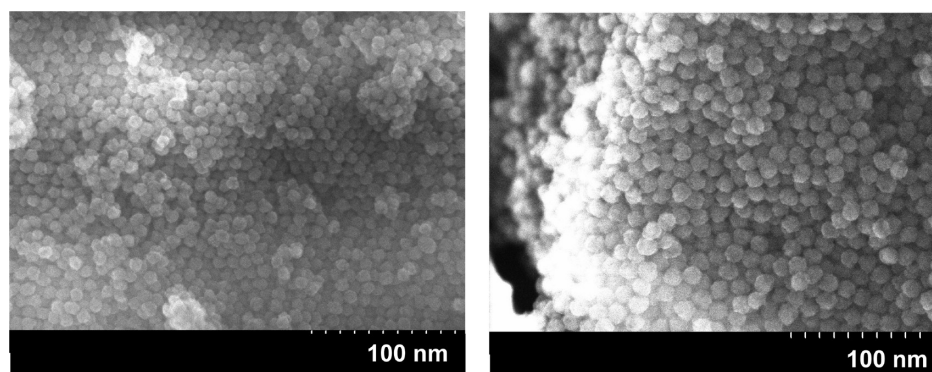

Figure 5. FE-SEM images of the SNSs prepared by the method A at $x = 2$ (left) and $x = 5$ (right), followed by solvent evaporation. Scale bar: 100 nm.

3.2. Effects of Synthesis Conditions on Formation of SNSs. *3.2.1. Effect of Stirring Rates.* The effect of stirring conditions on the formation of SNSs was investigated. The reactions were conducted at 333 K for 24 h at the stirring rates of 0, 150, 550, and 950 rpm. The representative FE-SEM images of the solid products after the solvent evaporation are shown in Figure 4. The product synthesized without stirring is not uniform in size; the sizes range from 25 to 45 nm (Figure 4a). At the stirring rates of 150 and 550 rpm, relatively uniform, spherical particles 25−30 and 12−14 nm in size are formed, respectively (images b and c in Figure 4). When the stirring rate is further increased to 950 rpm, the size is decreased to 10 nm while keeping the uniformity (Figure 4d). The yields of the silica products after evaporation of solvents were 16, 33, 100, and 100% when the stirring rates were 0, 150, 550, and 950 rpm, respectively. The lower yields at the slow stirring rates are ascribed to the incomplete reaction of TEOS.

3.2.2. Effect of Composition of the Reactants. The SNSs were prepared with varying amounts of TEOS by two methods; one is the change in the initial amount of TEOS (method A) and the other is the stepwise addition of TEOS to the parent synthesis system after the reaction at 333 K for 12 h (method B). The FE-SEM observations of the solid products after the solvent evaporation reveal that all of the products consist of uniform-sized silica spheres. The sizes are 18 and 27 nm at $x = 2$ and 5, respectively (method A, Figure 5), and 27 and 35 nm at $y = 4$ and 10, respectively (method B, Figure 6). The relationship between the molar ratio of total TEOS introduced and the final size of the SNSs is shown in Figure 7. The increase in the amount of TEOS leads to the linear increase in the particle size regardless of the addition method of TEOS at least under our experimental conditions.

To examine the effect of the amount of lysine, we varied the lysine/TEOS molar ratio from 0.002 to 0.08. As we
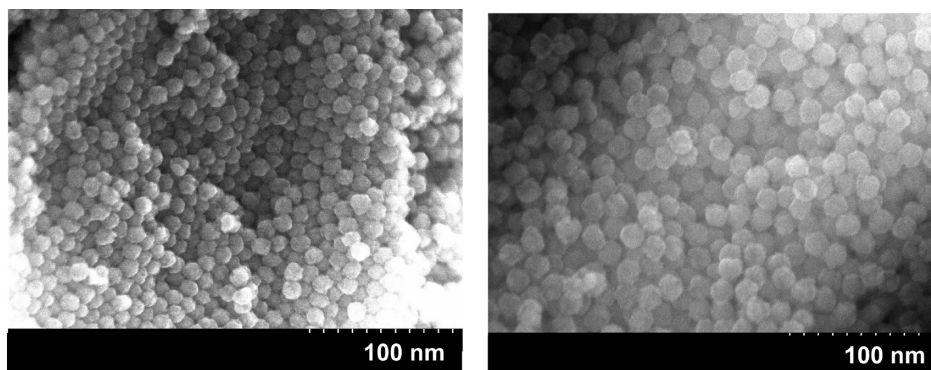
Figure 6. FE-SEM images of the SNSs prepared by the method B at $y = 4$ (left) and 10 (right), followed by solvent evaporation. Scale bar: 100 nm.
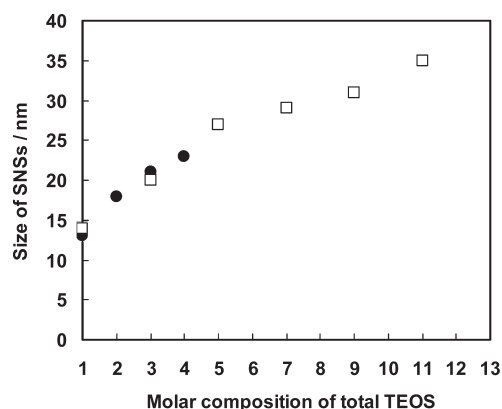

Figure 7. Relationship between the molar ratio of total TEOS introduced and the final size of the SNSs. Filled circles: method A; open squares, method B.

Figure 8. Relationships between the change in the pH of the synthesis system of (a) our and (b) the Stöber methods and the weight loss of the solvent upon the evaporation process.

reported recently,[20] the increase in the amount of lysine led to an increase in the pH of the starting emulsion (water phase) from pH 8.4 to 10.2. The FE-SEM observations of the products after the solvent evaporation (data not shown) revealed that uniform-sized SNSs were formed and that their size was decreased with an increase in the amount of lysine; when the molar ratio of lysine was 0.002 and 0.08, the sizes were 25 and 8 nm, respectively.

We also examined the effect of the addition of EtOH on the formation of the SNSs. The reaction was performed at the molar composition of 1TEOS: 0.02lysine: $(162 - m)$ H$_2$O: mEtOH ($m = 0 - 100$). No significant difference was observed for the SNSs prepared at $m < 50$ (data not shown). However, further increases in the EtOH amount ($70 < m$) resulted in steep increases in the particle size (see the Supporting Information, Figure S1), which would be due to the partial homogenization of the emulsion. The detailed effect of cosolvent on the formation of SNSs is currently being studied and will be reported elsewhere.

3.3. Changes in Zeta Potential and pH during Evaporation Process. The solvent evaporation process leading to the solid SNSs with a cubic closed-packed (ccp) structure was investigated.[19] The zeta potential (z) was kept constant at approximately -40 mV throughout the evaporation process. The relationship between the pH value and the weight loss of the dispersions during the evaporation is displayed in Figure 8a. The pH value is almost unchanged at pH 9.4 during the evaporation. Interestingly,
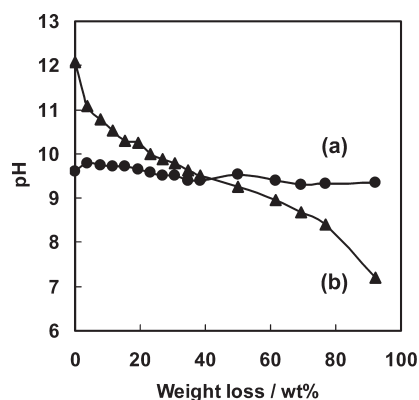
the sedimentation of the SNSs did not occur until more than 90 wt % of the solvent was evaporated.

On the other hand, in the Stöber method, the pH value was gradually decreased during the evaporation (Figure 8b). The z value has also changed along with evaporation; when 0, 50, and 80 wt % of the solvent were evaporated, the z values were approximately -65, -40, and -23 mV, respectively.

3.4. Location and State of Lysine. The location and chemical state of lysine molecules should be identified to elucidate the role of lysine in the formation and assembly of the SNSs. The liquid-sate ^{13}C NMR spectrum of lysine in an aqueous solution containing D$_2$O (pH 10.7) is shown in Figure 9a. C1, C2, C3, C4, C5, and C6 carbons (inset of Figure 9a) are observed at 184.2, 58.3, 42.2, 35.9, 30.2, and 24.5 ppm, respectively. Figure 9b shows the solid-state ^{13}C CP/MAS NMR spectrum of the powder of the SNSs collected by centrifugation followed by air-drying, confirming that a certain amount of lysine was contained in the sample. The signals at 176.7, 55.7, 40.5, 32.1, 27.7, and 22.7 ppm are assigned to the C1′, C2′, C3′, C4′, C5′, and C6′ carbons of lysine (inset of Figure 9b), respectively. Two large signals at 59.4 and 17.8 ppm are assigned to ethoxy groups, which might be formed by esterification of surface SiOH groups with ethanol derived from TEOS.[42] All of the carbon signals of lysine in

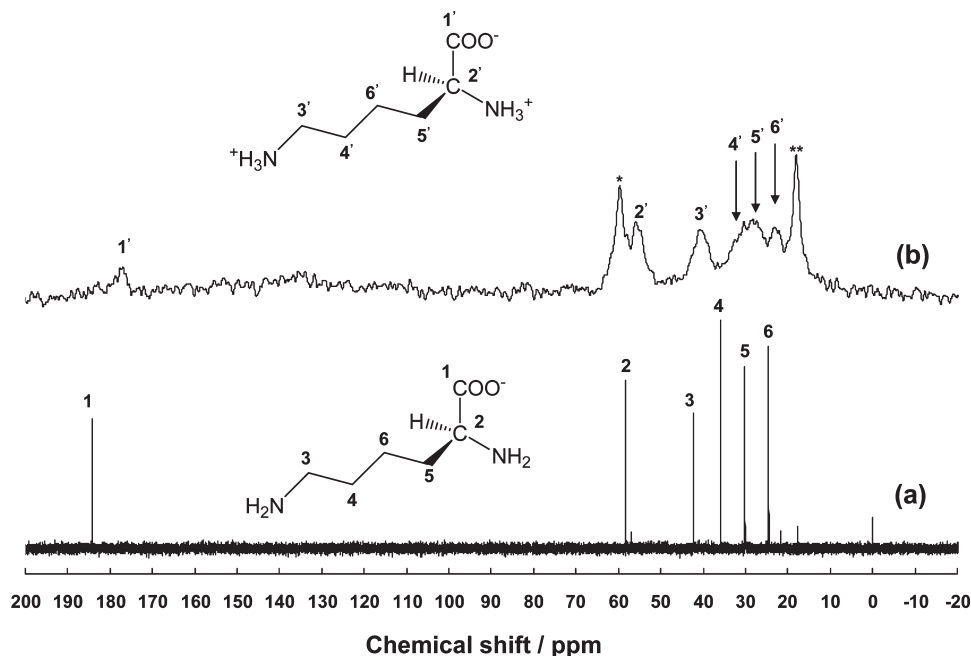(42) Shimojima, A.; Goto, R.; Atsumi, N.; Kuroda, K. *Chem.—Eur. J.* **2008**, *14*, 8500–8506.

Figure 9. (a) Liquid-state ^{13}C NMR spectrum of the aqueous solution of lysine. The small signals at 0, 17.5, 21.7, and 56.9 ppm are due to the internal standard (sodium 3-(trimethylsilyl)-1-propanesulfonate) used for the measurement. (b) Solid-state ^{13}C CP/MAS NMR spectrum of the powder of the SNSs collected by centrifugation (* and ** peaks at 59.4 and 17.8 ppm are assigned to the ethoxy groups).

the powder sample (C1′−C6′) are observed further upfield than those of lysine in the aqueous solution (C1−C6), suggesting that the chemical states of lysine are quite different between these samples. Such upfield shifts (2−4 ppm) of C-NH$_2$ signals are indicative of the protonation of amino groups (C-NH$_3^+$).[43]

The TG-DTA curves of the SNSs after solvent evaporation are very similar to those for the physical mixture of the calcined SNSs and lysine (see the Supporting Information, Figure S2), suggesting that lysine molecules were present on the surface of the SNSs, not occluded inside the spheres. If lysine molecules are occluded inside the silica spheres, their combustion should be hindered and then the related peaks should shift to higher temperatures or disappear. Furthermore, the amount of lysine molecules adsorbed on the surface of the SNSs was estimated by analyzing the powder samples collected by centrifugation. By combining CHN elemental analysis and TG, the molar ratio of lysine/SiO$_2$ was calculated to be ca. 0.01, which is about half of the initial lysine/TEOS ratio (0.02).

4. Discussion

4.1. Formation Mechanism of Uniform-Sized SNSs. Two major mechanisms have been proposed to account for the formation of uniform-sized particles in solutions. In the 1950s, the so-called "LaMer mechanism" was proposed.[44] This mechanism is based on a short burst of nuclei that generates all of the particles observed at the end of the reaction. After nucleation stops, the particles

continue to grow by the addition of monomer species onto the surface of the particle until an equilibrium concentration, and uniformity in size is achieved through a self-sharpening growth process.[45] On the other hand, the continuous nucleation/aggregation mechanism has been proposed by Bogush and Zukoski; a nucleation occurs continuously throughout the reactions and nuclei or primary particles aggregate with one another or with larger aggregates.[46]

It was confirmed by the FE-SEM observations that the SNSs ca. 4 nm in size were formed after 0.5 h of the reaction. If the formation of SNSs in the present system follows the continuous nucleation/aggregation mechanism, the change in the number density (*n*) should be observed. However, the results of the FE-SEM and SAXS measurements suggested that particle growth proceeded without forming new particles. The liquid-state NMR measurements revealed that the completion of the TEOS hydrolysis required a reaction time of 8 h, suggesting that silicate species derived from TEOS were slowly and continuously supplied. Such silicate species would be immediately consumed for the growth of the parent silica particles as stated below.

The slow hydrolysis of TEOS in our system is in clear contrast to the Stöber process, where colloidal dispersions are formed within several minutes. This is mainly attributed to the emulsion system consisting of TEOS, lysine, and water, where hydrolysis of TEOS should occur at the interface between the water (lysine and water) and the oil (TEOS) phases. The relatively moderate pH value

(43) Silverstein, R. M.; Webster, F. X., *Spectrometric Identification of Organic Compunnds*, 6th ed.; John Wiley & Sons: New York, 1999.
(44) (a) LaMer, V. K.; Dinegar, R. H. *J. Am. Chem. Soc.* **1950**, *72*, 4847–4854. (b) LaMer, V. K. *Ind. Eng. Chem.* **1952**, *44*, 1270.
(45) Matsoukas, T.; Gulari, E. *J. Colloid Interface Sci.* **1991**, *145*, 557–562.
(46) (a) Bogush, G. H.; Zokoski, C. F. *J. Colloid Interface Sci.* **1991**, *142*, 1–18. (b) Bogush, G. H.; Zokoski, C. F. *J. Colloid Interface Sci.* **1991**, *142*, 19–34.
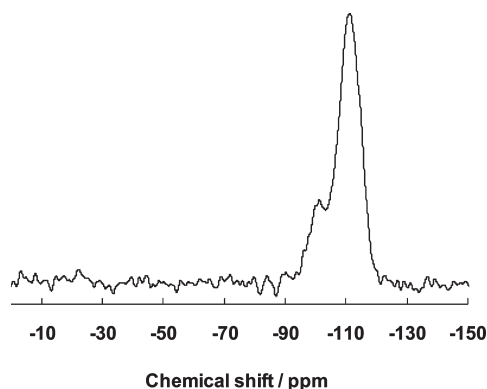
Figure 10. ^{29}Si MAS NMR spectrum of the SNSs obtained by the solvent evaporation. The peaks at −101 and −109 ppm correspond to the Q^3 and Q^4 silicons ($Q^n = Si(OSi)_n(OH)_{4-n}$), respectively, with the integral intensity ratio of $Q^3/Q^4 = 0.26$.

of the water phase (pH 9−10) is also responsible for the slow hydrolysis of TEOS. It is known that hydrolysis rate of TEOS is drastically decreased as the pH of the reaction media becomes closer to neutral, whereas the condensation rate of silicate species is increased.[1] In addition, the solubility of silicate species is low at pH 9−10.

The solid-state ^{29}Si MAS NMR spectrum of the SNSs obtained by the solvent evaporation (Figure 10) shows the peaks corresponding to the Q^3 and Q^4 silicons ($Q^n = Si(OSi)_n(OH)_{4-n}$). The Q^3/Q^4 ratio is calculated to be 0.26, suggesting that a number of $\equiv$Si−O$^-$ or $\equiv$Si−OH sites are located on the surface of the SNSs. The silicate monomers and oligomers barely supplied from the oil−water interface can immediately react with $\equiv$Si−O$^-$ or $\equiv$Si−OH groups on the surface of the particles, leading to the growth of SNSs. It is plausible that diffusion-controlled growth is more dominant than the reaction-controlled growth.

In conclusion, both the TEOS−lysine−water emulsion system and weakly basic conditions are key factors for the formation of the SNSs. Although the whole formation mechanism has still been unclear, the growth mechanism can be explained by the diffusion-controlled addition of monomer species on primary particles.

4.2. Effects of Various Synthesis Conditions on Formation of SNSs. *4.2.1. Effect of Stirring Rate.* The stirring rate greatly affects the uniformity as well as the size of the SNSs because the hydrolysis of TEOS in the emulsion system occurs at the interface between the water and the oil phases. The fast stirring enhances the hydrolysis rate of TEOS, leading to the formation of more silica particles at the initial stage of the reaction. Consequently, the smaller-sized SNSs were obtained. On the contrary, the slow stirring retards the hydrolysis of TEOS in the emulsion system, resulting in the formation of larger-sized SNSs with a low yield. Moreover, the growth of the parent particles under the static conditions would heterogeneously proceed resulting in different-sized SNSs.

4.2.2. Effect of Molar Ratio of TEOS. The uniform-sized SNSs. 12 nm in size were formed after the reaction time of > 8 h. Therefore, the following question arises:

"Does additional TEOS contribute to further growth of the "pre-formed" spheres or to the formation of new silica spheres?" In the former case, the sphere size will be increased. In the latter case, the uniformity in the sphere size will be lowered. In the method B, based on the stepwise addition of TEOS, the increases in the TEOS ratio resulted in the increases in the particle size, whereas the uniformity was unchanged. It is therefore concluded that the additional TEOS contributed to the further growth of the preformed SNSs, not to the formation of new silica particles; the preformed SNSs acted as the "seed".

We note here that when TEOS was added in one-step from the beginning of the reaction (method A), the increase in the initial amount of TEOS should affects the supply rate of silicate species into the water phase due to the change in the oil−water interfacial area. This might cause the difference in the number density of primary particles. However, at least under our experimental conditions, the relationship between the total TEOS ratio and the resulting particle size was very similar to that observed for the method B.

Such a "seed regrowth method" has been originally claimed for the size control of the Stöber silica spheres.[47,48] Because the pH of the synthesis system was unchanged (pH 9−10) throughout the reaction of TEOS, the hydrolysis rate of TEOS was not raised but the condensation of silicate species would be very fast. Under such conditions, it is likely that incremental silicate species are consumed for further growth of preformed SNSs by condensation with surface silanol groups rather than for the formation of new silica particles, which is consistent with the monomer addition mechanism.

4.2.3. Effect of Molar Ratio of Lysine. A decrease in the molar ratio of lysine resulted in a decrease in the pH and an increase in the size of the SNSs. Under the lower pH conditions, silicate species are more slowly supplied to the water phase because of a lower hydrolysis rate of TEOS, which should result in a decrease in the number of primary particles and therefore an increase in the final size of the SNSs. On the contrary, pH is increased along with the amount of lysine. The increase in pH enhances the hydrolysis rate of TEOS, producing more silicate species at the initial stage of the reaction. Such conditions should lead to an increase in the number of primary particles, resulting in a decrease in the final size of the SNSs.

4.3. Adsorption of Lysine on SNS's Surface. Our experimental results suggested that about half of lysine molecules in this system were adsorbed on the surface of SNSs. Considering the pH value of the dispersion (ca. pH 9.4) and dissociation constant of lysine,[49] ca. 92% of C3-NH$_2$ and 33% of C2-NH$_2$ groups in lysine molecule would be protonated. Actually, the ^{13}C CP/MAS NMR

(47) Giesche, H. *J. Eur. Ceram. Soc.* **1994**, *14*, 205−214.
(48) Chang, S. M.; Lee, M.; Kim, W.-S. *J. Colloid Interface Sci.* **2005**, *286*, 536−542.
(49) McKee, T.; , McKee, J. R.; , Biochemistry; The McGraw-Hill Companies: New York, 2003.

spectrum of the SNSs collected by centrifugation indicates that parts of C2-NH$_2$ and C3-NH$_2$ groups are protonated, as mentioned above (see section 3.4). It is therefore likely that lysine molecules are attached to the surface of SNSs by electrostatic interaction between $-NH_3^+$ groups and de-protonated silanol groups.

Assuming that all of TEOS was consumed for the formation of spherical SNSs (theoretical density of 2.2 g cm^{-3}) with the diameter of 12 nm, it is estimated that lysine molecules are attached on the surface of the SNSs with a surface density of ca. 0.5 nm^{-2}. Note that the theoretical surface area ($\sim$230 m^2 g^{-1}) based on these assumptions (shape, size, and density of SNSs) is in good agreement with the BET surface area of the SNSs after the evaporation and calcination measured by nitrogen adsorption (228 m^2 g^{-1}). On the other hand, it is assumed that the surface density of Si$-$O$^-$ (or SiOH) groups on the external surface is 3 nm^{-2}.[50] From these values, the fraction of the surface Si$-$O$^-$ (or SiOH) groups that are interacted with lysine molecules can be estimated to be 15%.

4.4. Mechanism of Regular Arrangement of SNSs upon Evaporation. The SNSs are regularly arranged into a cubic closed-pack (ccp) structure upon the solvent evaporation.[19] The last issue is why "three-dimensionally ordered" SNSs can be obtained.

When the reaction of TEOS is performed in the emulsion system containing TEOS, water, and ammonia with the molar composition of 1 TEOS: 0.02 NH$_3$: 162H$_2$O, the pH of this mixture was 9.4, which is almost identical to that of the standard TEOS$-$lysine$-$H$_2$O system. However, the product after the solvent evaporation is aggregates of silica particles 8$-$10 nm in size without any regularity (see Figure S3 in the Supporting Information). This fact suggests that even though silica nanospheres are formed, the well-ordered structure cannot be attained simply by adjusting the pH of the system (pH 9$-$10), implying the crucial role of basic amino acids in our system.

The zeta potential is due to the overall charge that a particle acquires in a specific solvent, and its magnitude gives an index of the stability of the colloidal system.[51] If all the particles have a negative or positive large z, they repel each other. A dividing border between stable and unstable aqueous dispersions is generally taken at around $\pm$30 mV. The dispersions of SNSs prepared by our and the Stöber methods showed significant differences in the variations of z and pH values during the evaporation process. The dispersion prepared by our method had a constant pH value ($\sim$9.4) throughout the evaporation process, which is attributed to the buffering action of

basic amino acids. This constant pH value should explain the constant z value (-40 mV) in this system. On the other hand, in the Stöber method, the z value was changed from -65 to -23 mV, which is possibly due to the decrease in the pH value[51] caused by more rapid evaporation of ammonia than water. For these reasons, the dispersions prepared by our method are more stable than those obtained by the Stöber method during the evaporation process. If buffering action is not operative, change in the pH and z values should cause aggregation of the SNSs as in the case of the Stöber method.

Wang et al. also reported that silanol groups on the external surface of silica particles enhance the repulsion between the particles, leading to the assembly of well-ordered colloidal crystal, not aggregation of the particles.[52] Similarly, uniform-sized latex beads with surface charges can form ordered two or three-dimensional arrays.[53] In our system, in addition to surface silanol groups, protonated lysine molecules are present on the external surface. Strong repulsion effect due to the lysine molecules in addition to uncovered surface silanol groups could be operative during the reaction and evaporation processes. The repulsion effect and colloidal stability would be the necessary conditions for the formation of the well-ordered assembly. We also speculate that attractive interaction due to hydrogen bonding between the basic amino acids might be operative at the final stage of the evaporation.

5. Conclusions

The formation mechanism of uniform-sized and well-ordered SNSs was discussed on the basis of the results of FE-SEM, SAXS, and liquid-state NMR measurements. The key factors for preparing the SNSs are the weakly basic conditions and the emulsion system. The basic amino acids act as (i) a weak base catalyst to achieve slow hydrolysis of TEOS and (ii) a buffer to keep the pH value constant during the synthesis. The buffering action is also exercised during the evaporation process to prevent random aggregation of the SNSs and to achieve their well-ordered arrangements. The size of the SNSs was successfully controlled by varying the stirring rates and/or the composition of the reactants. The precise control and further extension of the sphere size and the assembled structure are currently being studied and will be reported elsewhere.

(50) (a) Shenderovich, I. G.; Buntkowsky, G.; Schreiber, A.; Gedat, E.; Sharif, S.; Albrecht, J.; Golubev, N. S.; Findenegg, G. H.; Limbach, H.-H. *J. Phys. Chem. B* **2003**, *107*, 11924–11939. (b) Shenderovich, I. G.; Mauder, D.; Akcakayiran, D.; Buntkowsky, G.; Limbach, H.-H.; Findenegg, G. H. *J. Phys. Chem. B* **2007**, *111*, 12088–12069.
(51) (a) Derjaguin, B. V.; Landau, L. *Acta Physicochim.* **1941**, *14*, 633. (b) Verwey, E. J. W.; Overbeek, J. T. G. Theory of the Stability of Lyophobic Colloids; Elsevier: Amsterdam, 1948.(c) Visser, J. In Surface and Colloid Science; Wiley: New York, 1976.

(52) Wang, W.; Gu, B.; Lang, L.; Hamilton, W. *J. Phys. Chem. B* **2007**, *107*, 3400–3404.
(53) Zeng, F.; Sun, Z.; Wang, C.; Ren, B.; Liu, X.; Tong, Z. *Langmuir* **2002**, *18*, 9116–9120.

Article

Chem. Mater., Vol. 21, No. 15, 2009 3729

Supporting Information Available: Details of experimental procedures and additional data (PDF). This material is available free of charge via the Internet at http://pubs.acs.org